



## Comparative Study Between Synergetic Control and Sliding Mode Control using MPPT Techniques

**Khokha Bouguerra<sup>a,\*</sup>, Samia Latreche<sup>a</sup>, Hamza Khemliche<sup>b</sup>, Mabrouk Khemliche<sup>a</sup>**

<sup>a</sup> *Electrical Engineering Department Ferhat Abbas Setif 1 University-UFAS, Setif, Algeria*

<sup>b</sup> *Research Centre in Industrial Technologies-CRTI, P.O. box 64, Cheraga 16014, Algiers, Algeria*

### ARTICLE INFO

#### Article history:

Received September 30, 2024

Accepted October 21, 2024

#### Keywords:

Photovoltaic system faults,  
Synergetic control,  
Sliding mode control,  
DC-AC converter,  
DC/DC boost converter.

### ABSTRACT

Researchers are focusing on extracting maximum energy from photovoltaic cells due to non-linear characteristics like solar radiation, temperature, carrier, misdirection, and internal current. Advanced DC-Link controllers and current controllers, DC/DC boost converter, MPPT controller, DC-AC inverter phase reactive power compensation operation, synchronization and current grid supply are required. Synergetic control SC is introduced as a new tool in PV control, and we compared it with sliding mode control SMC stands out as a powerful and effective tool. We have implemented techniques such as sliding mode-based MPPT controller and synergetic control SC to allow us to conduct a general study and a comprehensive, taking into account factors such as efficiency, complexity and response time. SC algorithms show efficiency and superiority over MPPT-SMC algorithms in terms of stability, efficiency, speed of response, and maximum power point output without chattering. A PV Grid-Connected System model was created at Simulink to confirm the effectiveness of the proposed global synergistic control mechanism.

## 1. INTRODUCTION

It has become necessary to find solutions to meet the global demand for electricity, the increasing demand and the problem of pollution have led to the search for alternatives that allow increasing electricity production. These complexities help to clarify solar energy in particular as well as renewable energies in general. Due to its infinite heat and pure state, solar energy has become a crucial means of generating energy. Recent years have seen significant advances in the technology used to capture solar radiation and convert it into electricity. The sun is considered an endless source of Infinite Energy and can be used reverently, and for a long time. Solar panels using photovoltaic technology collect this negative energy (*D'Souza et al. 2010*). Over ten years, interest in photovoltaic systems has grown due

\* *Corresponding author, E-mail address: [khaoukha.bouguerra@yahoo.com](mailto:khaoukha.bouguerra@yahoo.com)*



to their benefits, including clean, noiseless, and easy installation. Advancements in electronics and computer tools have contributed to this growth. Algeria, with its large Saharan surface, has high export potential for solar electric energy. Industrial and economic growth in the world is significantly influenced by energy. Many governments have provided funding for renewable energy projects in response to the recent increase in fuel prices and energy demand. But electricity system operators are now facing additional difficulties due to the unpredictability of these supplies, the analysis of contemporary energy systems is essential to address these issues and ensure effective integration of renewable energy. Two critical components must be included for the development of this energy system: renewable energies at the production level and a smart grid at the management level. This will provide security, stability, reliability and energy quality.

An MPPT controller is necessary to extract the most power since PV systems output Due to temperature and irradiance changes, properties are nonlinear. In order to guarantee that the PV operates at its MPP, the MPPT techniques are used (*Bouguerra & Bendifla, 2023*). When combined with mechanical tracking, MPPT maximizes the power generated by solar PV modules with a particular algorithm and control system (*Bait et al., 2022*). To use MPPT, a DC-DC converter is required. By modifying the duty cycle, the maximum power from the photovoltaic module is sent to the load using a DC-DC converter our Grid (*Ahmad et al. 2020*). The goal is to integrate solar energy into the AC grid by increasing the low voltage generated by the panels to a level suitable for conversion and grid integration. A single-phase grid-connected photovoltaic power system has only one switching phase, this switching phase is a DC-AC converter used to extract maximum power from photovoltaic panels and supply it to the network at the same time. The inverter must first convert the DC power of the boost transformer into AC power before it can be put into the grid because the solar panels produce DC power and the AC grid runs on AC power.

The literature has studied a number of methods, including perturb and observe (P&O) for finding the MPP of solar systems (*Jain et al., 2018*). The complexity, reaction time, cost of implementation, accuracy, and other factors of these techniques differ. However, in quickly shifting atmospheric circumstances, they may not be able to reach MPP. In the literature, unconventional techniques have also been employed (*Bait et al. 2022*), including fuzzy logic controllers (FLC) and sliding mode controllers (SMC) and Synergetic Nonlinear Controller (SNC) (*Bouguerra & Bendifla, 2020; Kazmierkowski & Sobczuk, 1996*).

The use of Fuzzy Logic has become very widespread recently, that an excellent performances and immunity to disturbances. In addition, he SMC is a popular nonlinear control method. For this reason, are preferred since they are more accurate than other conventional procedures and have better clarity and durability. However, the issue of chatter, which leads to undesirable oscillations, is its worst drawback (*Haji & Genc, 2018; Pradhan & Subudhi, 2016; Taissala et al. 2022*).

The literature also recommended synergetic control SC as a potential solution to this problem. One benefit of the Synergetic Controller is that it guarantees a fast-dynamic response and strong resilience, especially when oscillations are not present. A nonlinear control approach is Synergetic Control, also known as Slide Mode Control (*Jain et al., 2018*). The benefits of the synergetic controller are low steady-state error and quick time convergence.

The structure of the document is as follows. In Section 2, a brief review of the modelling of solar systems is presented. In Section 3, the MPPT-SMC and MPPT-SC synergistic control methods for sliding mode controllers are disclosed. Section 4 In this section we present the results obtained and in the fifth and last section we present the conclusion

## 2. THOUGHTFUL SYSTEM ANALYSIS

Fig. 1 shows the composition of the system we will present in this research. The Transformer DC-constant current is powered by MPPT technology, which increases the overall energy efficiency of the system. This power is supplied by a DC/AC transformer, which is controlled by an RL filter for harmonic current reduction and a voltage-guided control system (VOC) for independently regulating active and reactive forces (Jain et al., 2018).

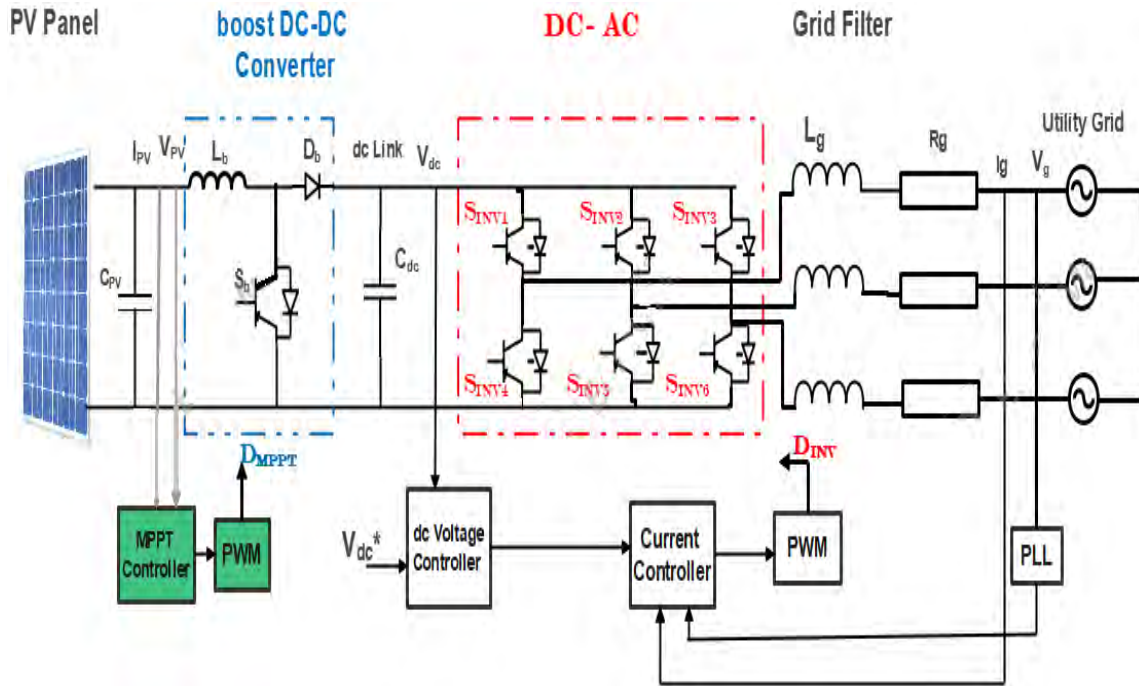


Fig 1. Grid-connected photovoltaic system

### 2.1 PV system Description

According to Fig. 2, the general photovoltaic system consists of four necessary elements. The photovoltaic panel represents the receiving element of solar rays and converts them into the primary mass current, the second block is a static DC converter, the third element is represented in pregnancy. The fourth element is the control system. The main purpose of the transformer is to match the impedance so that the panel provides the greatest amount of power possible.

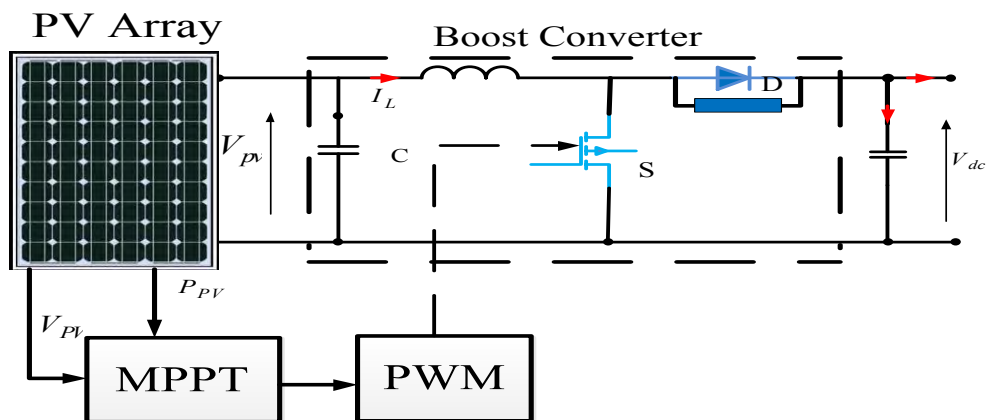


Fig 2. The diagram shows a PV system using maximum power point tracking technology

### 2.1.1 Photovoltaic modeling

Fig. 3 represents the electrical model of photovoltaic cell with one diode.

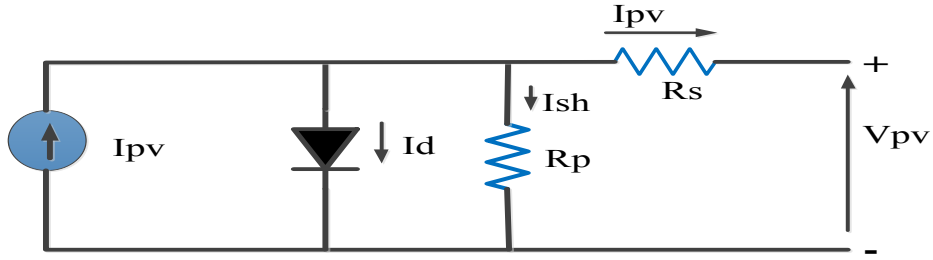


Fig 3. Solar cell

The general mathematical equation for a PV cell is as follows:

$$I = I_{pv}N_P - I_d - I_{sh} \quad (1)$$

$I_{ph}$  is a stream of light. The diode's current is called,  $I_d$  while the shunt current is called the  $I_{sh}$ . The following is the equation for photovoltaic current

$$I_{pv} = I_{sc} + K_i(T - 298) \frac{G}{1000} \quad (2)$$

The current conversion equation gives the following form

$$I_{sh} = \frac{V_{pv} + I_{pv}R_s}{R_p} \quad (3)$$

The solar diode equation is given as follows

$$I_d = I_s \left[ \exp \left( q \frac{V_{pv} + R_s I_{pv}}{N_s V_t} \right) - 1 \right] \quad (4)$$

The following equation shows reserved saturation current changes with temperature:

$$I_0 = I_{sh} \left( \frac{T}{T_n} \right)^3 \exp \left[ \frac{qE_{g0} \left( \frac{1}{T_n} - \frac{1}{T} \right)}{nK} \right] \quad (5)$$

In another level, the output current dependence is given as follows:

$$I = I_{pv} - I_0 \left[ \exp \left( \frac{q(V + IR_s)}{nKN_s T} \right) - 1 \right] - I_{sh} \quad (6)$$

Where  $V_{oc}$  Open circuit voltage,  $R_s$  Series resistance,  $R_p$  Shunt resistance, and  $V_t$  for the module's thermal voltage:  $V_t$  is equal to  $N_s KT/q$ .  $T$  is the cell's temperature;  $q$  is the electron charge, which is equal to  $1.6 \cdot 10^{-19}C$ ;  $K$  is the Boltzmann constant, which is equal to  $1.3854 \cdot 10^{-23} J/^{\circ}K$ ; and  $n = 1.3$ , the diode ideality factor which is between 1 and 2.

### 2.1.2 Simulation

In order to understand the influence of environmental factors such as temperature, solar irradiance, dust accumulation, tilt angle direction, misdirection effect and internal factors, we conducted simulations

using Matlab/Simulink . And the results of the tests are presented in Figure 4 to figure 8, in different conditions of temperature, irradiance and change in the rectifiers of the photovoltaic panel.

Table 1. The PV module's settings

Parameters	Symbols	Values
Rated power of panel PV	Pmp	40W
Voltage at MPPT	Vmp	18.24V
Current at MPPT	Imp	2.20A
Voltage of open-circuit condition	Voc	21.28V
Current of short-circuit condition	Isc	2.35A
Number of series cells in solar PV	Ns	36

• **Irradiance effect:**

Fig. 4 shows the properties of an electric cell under a variation in irradiance of several values (1200, 1000, 800, 600, 400) while the temperature is maintained at 25°C. Little voltage changes and The more radiation we observe an increase in the power generated by the solar system

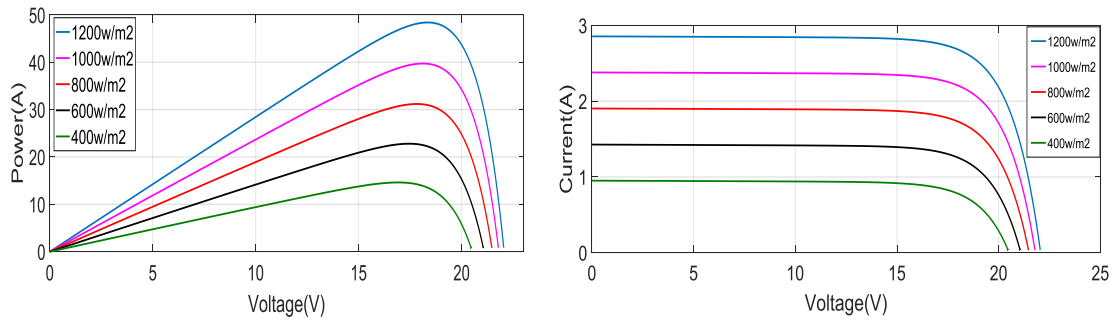


Fig 4. Study examining the effects of a change in sunlight (T=25C°)

Table 2. Photovoltaic cell performance for different sunlight intensity

Irradiance (W/m2)	400	600	800	1000	1200
Maximum power point MPP (W)	14.672	23	31.2	40	48.5
Open-circuit voltage Voc (V)	20.46	21.463	21.514	21.28	22.041
Short-circuit current Isc (A)	0.954	1.431	1.912	2.35	2.85

• **Temperature effect:**

In order to understand the characteristics of the photovoltaic cell we made a temperature change (0, 15, 25, 35, 45C°) and irradiance stabilization at 1000W/m2. Where we observe an array increase in current at higher temperature and a decrease in voltage due to an increase in Isc and as a result the resulting energy decreases (Fig. 5).

• **Change in serial resistance:**

Fig.6 shows the effect of a change in the serial resistance (0.2, 0.5, 0.9, 2 Ω) the extent of its impact on the resulting ability with a diaper on the same current and voltage. Its effect in the slope of the curve is very obvious.

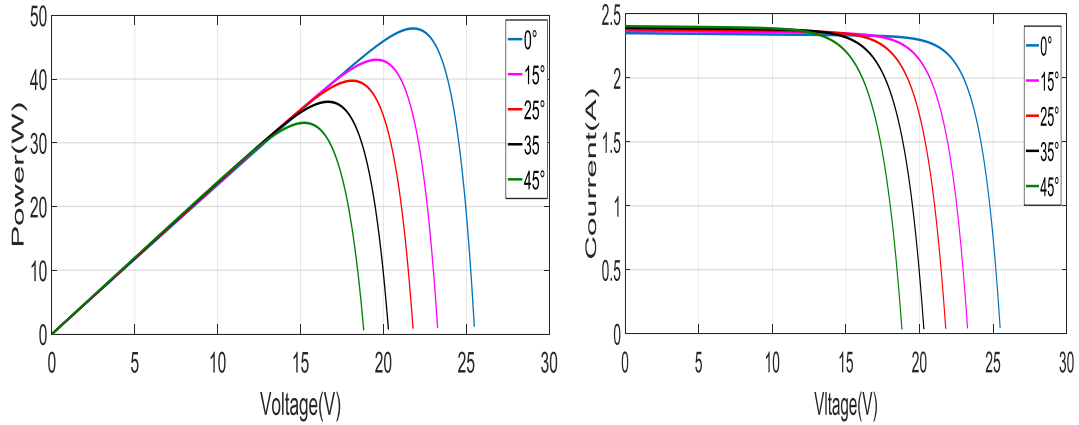


Fig 5. The effect of temperature on current, tension and power

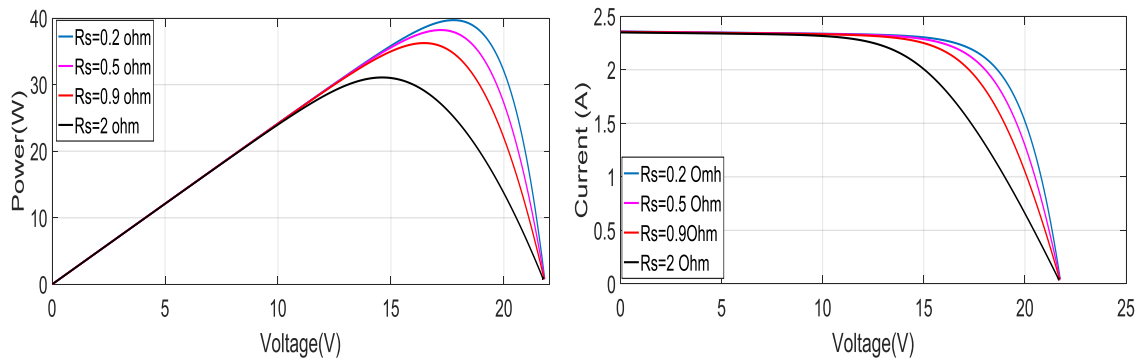


Fig 6. P-V and I-V characteristics under series resistance variation

Table 3. Outcomes of PV modules with different series resistance

Series Resistance ( $\Omega$ )	0.2	0.5	0.9	2
Maximum power point MPP (W)	40	38	36.75	31.09
Open-circuit voltage $V_{oc}$ (V)	21.28	21.2612	21.245	21.2031
Short-circuit current $I_{sc}$ (A)	2.4295	2.4287	2.4277	2.425

• **Variation of shunt resistance:**

The graphs in Fig. 7 illustrate the impact of shunt resistance fluctuation on the photoelectric property for various values (5, 8, 15, 950 $\Omega$ ). Power loss is caused by low shunt resistors (5, 8, 15 $\Omega$ ), which also lowers the values of  $I_{sc}$  and  $V_{oc}$ .

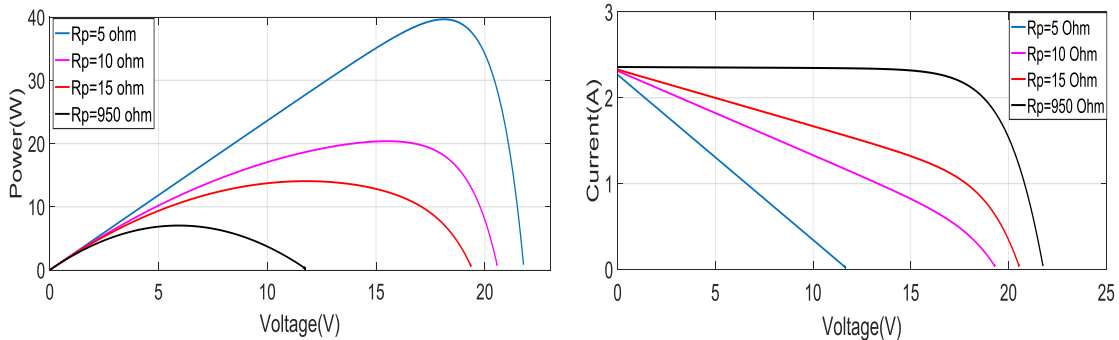


Fig 7. P-V and I-V characteristics under series resistance variation

Table 4. PV Module results for varying series resistance

Shunt resistance ( $\Omega$ )	5	10	15	950
Maximum power point MPP (W)	7.75	14.5	20.567	40
Open-circuit voltage Voc (V)	11.75	19.375	20.567	21.28
Short-circuit current Isc (A)	2.2105	2.245	2.98	2.35

### 2.2. Power conversion structure

A boost converter is necessary for photovoltaic systems. The MPPT controller is used to maintain the maximum output power at a constant value. In Fig. 8, a boost converter appears.

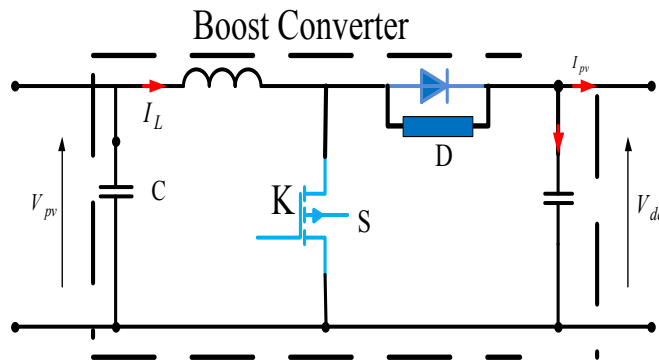


Fig 8. Circuit diagram of the boost converter

In solar systems, the use of DC converters is a must. The use of phase modulation between the solar panel array and the load allows extracting as much energy as possible at all times. It is possible to raise the photoelectric input voltage to the necessary output voltage using a DC-DC boost transformer as the interface between the two parts (Amara et al. 2020).

$$\begin{aligned} V_{pv} &= L \frac{dI_L}{dt} + V_{dc}(1 - K) \\ (1 - K)I_L &= C \frac{dV}{dt} + I_{ch} \end{aligned} \tag{7}$$

$$\begin{cases} \frac{dI_L}{dt} = \frac{V_{pv} - V_{dc}}{L} + \frac{V_0}{L} K \\ \frac{dV_{dc}}{dt} = \left( -\frac{V_{dc}}{RC} + \frac{I_L}{C} \right) - \frac{I_L}{C} K \end{cases} \tag{8}$$

$$x = x[x_1 \ x_2]^T = [I_L \ V_{dc}]^T$$

### 2.3. DC-AC Conversion System

The purpose of the DC-AC system is to convert produced by the solar generator into one- or three-phase alternating current. With the use of a continuous-alternative converter, one may convert a continuous voltage source into an alternate voltage with amplitude and frequency adjustments possible.

The power circuit of the voltage source inverter (VSI) with two levels is displayed in Fig. 9. It uses six bi-directional switches; each bidirectional switch consists of an IGBT with a parallel diode, to prevent the DC bond from shorting out, the two switches on each branch of the inverter must function in complimentary mode. Switches and diodes are thought to be the perfect gadgets.

The following formula may be used to define the inverter's output voltage in terms of switching states and DC continuous bus voltage:

$$\begin{aligned} V_A &= T_1 V_{dc} \\ V_B &= T_2 V_{dc} \\ V_C &= T_3 V_{dc} \end{aligned} \tag{9}$$

$$V = \frac{2}{3} (V_{aN} + \alpha V_{bN} + \alpha^2 V_{cN}) \tag{10}$$

$V_A, V_B, V_C$  : are the phase-neuter voltage N of the converter V

$T_1, T_2, T_3$  : are the commutations of the converter

$V_{dc}$  : is the input voltage V of the convert

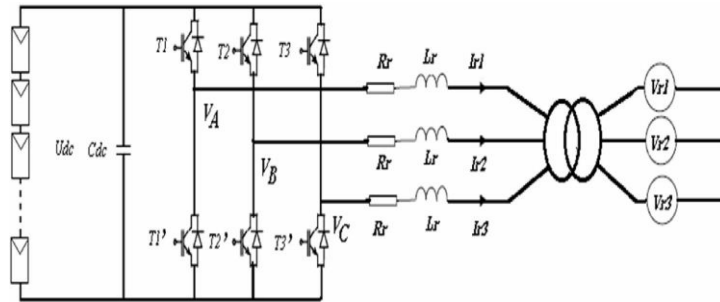


Fig.9. Triple voltage transformer

### 2.3. The proposed strategy of the inverter

The photovoltaic array acts as a current generator with a variable current characteristic I (V) (Jain et al. 2018). The task of the lifting transformer is to continuously follow the MPP and deliver it on board the continuous conveyor. The oscillator delivers power from the DC-DC converter to the network taking into account the current quality of the network.

- PI controller to regulate DC bus voltage.
- Hysteresis controller to control network currents and ensure high energy quality

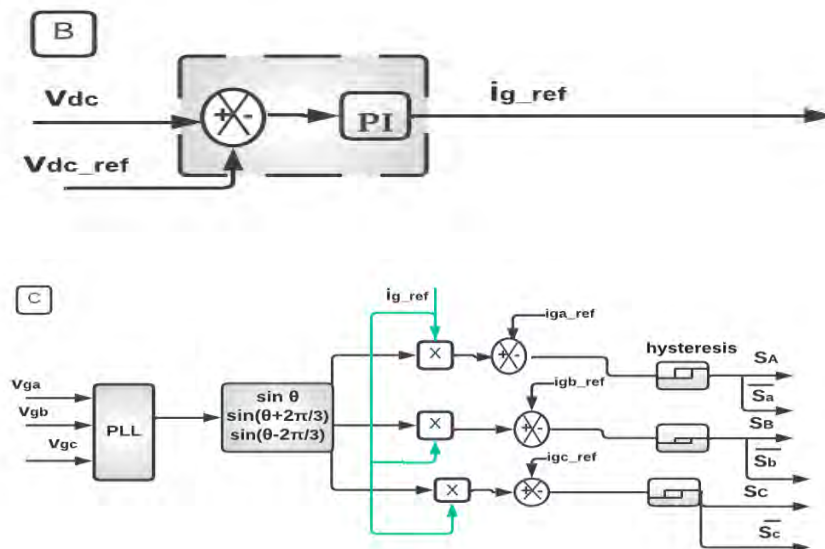


Fig. 9. (B) DC bus voltage management and (C) PLL control and hysteresis system

### 3. SLIDING MODE CONTROL DESIGN

There are two main aspects that sum up the aim of the sliding mode control:

- ✓ Develop a command rule that can draw all state trajectories to the sliding surface and keep them there.
- ✓ To make sure that each path in the system exhibits the desired behavior of follow-up, control and stability, create a surface  $S(x, t)$ .

Three primary phases are needed to design the regulators using sliding modes (*Bouguerra & Bendifla, 2023; Bait et al. 2022*).

- **Sliding surface chose**

Since the switch function is a scalar function, the variable that needs to be changed glides along this surface to the phase plane's origin. A generic form of equation was presented in (*Ahmad et al. 2020*) to find the sliding surface that guarantees a variable's convergence to its target value, which is defined as follows:

$$S(x) = e(x) + \lambda_m \frac{d}{dt} e(x) + \dots + \lambda_m \frac{d^m}{dt^m} e(x) \quad (11)$$

The control bandwidth is determined using where  $e(x)$  is a positive constant and  $m$  represents the comparative level  $\lambda_i$  ( $i = 1, 2, \dots, m$ ).

- **Convergence condition**

Convergence conditions are achieved in order to attach the sliding surfaces to the representative points of the trajectory of convergence.

The Conversion technique suggested by (*Haji & Genc, 2018*) and (*Taissala et al. 2022*) is recalled in this work and a sufficient appropriate condition can be used to formulate:

$$S(x) * \dot{S}(x) < 0 \quad (12)$$

In this condition, it is necessary to introduce for and its derivative, the just values to the left and to the right of commutation.

- **The conclusion of the law of control**

Two words form the basis of the law of control in the theories of the situation. The equivalent control law is the first term, it is calculated using  $\dot{s} = 0$ . In turn, the second limit is the law of commutative control, which depends on the signal of the sliding surface and can be written as follows:  $K_{sign}(S)$

$$U = U_{eq} + U_n \quad (13)$$

Thus, in order to keep the operating point in the switching surface and turn it towards the origin, it is necessary to ensure that the control variable is attractive to the sliding surface. This is related to the nonlinear component (*Bouguerra & Bendifla, 2020*).

The explicit control technique is required to guide the path used in the convergence mode to reach the sliding surface. It is called the "law of attack" strategy. And the definition of the law of access at a constant rate is:

$$U_n = -K_{eq} Sgn(S(x)) \tag{14}$$

Where,  $k_{eq}$  : the scaling factor, or (positive constant), is adjusted during the design phase to modify the step size.

### 3.1 Simulation results

The proposed control method works as intended, when the reference reactive energy and solar irradiance change (Fig. 10). The Matlab/Simulink program is used to conduct numerical simulations using the parameters listed in Table 1 and Table 5. The DC-DC adapter connecting the system to the DC bus is controlled using the MPPT approach. A DC-AC transformer controlled by voltage-guided control (VOC) is used to independently regulate active and reactive forces and an RL filter to lower the harmonic current to provide this power (Bouguerra & Bendifla, 2020).

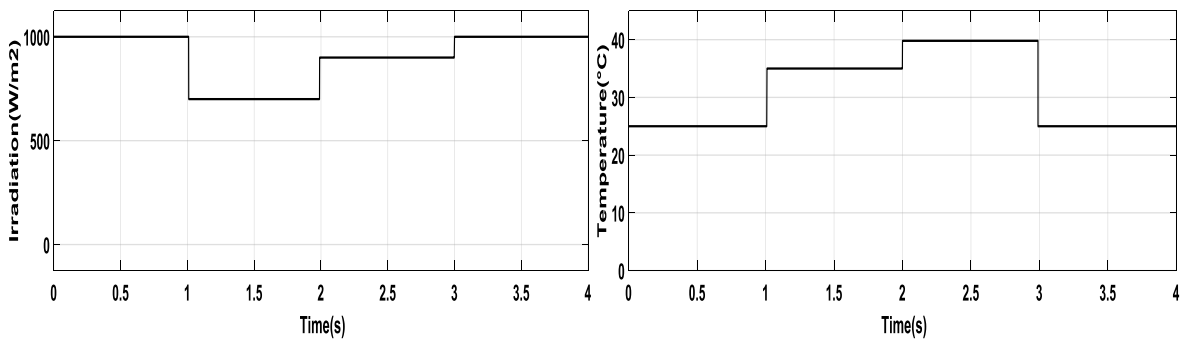


Fig 10. Change in solar irradiance and change in solar temperature

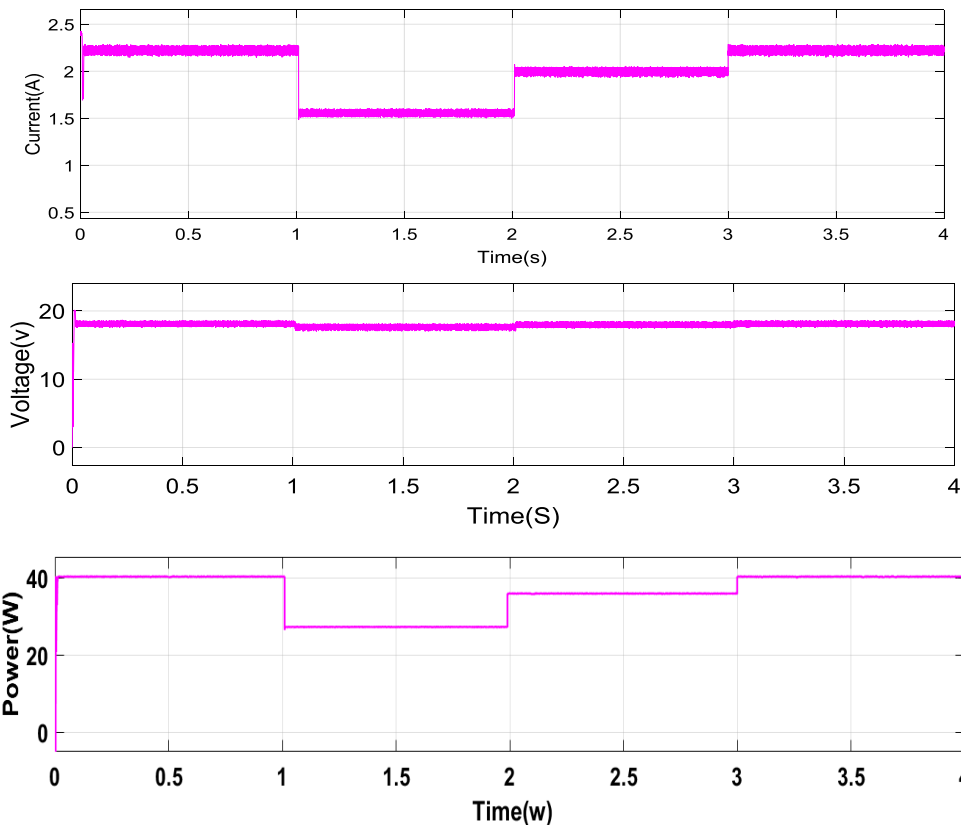


Fig 11. PV panel voltage and power current output under different levels of sunlight

Table 5. Details about power plants linked to the grid

Boost Converter	DC bus	PI	Filter	Grid	PV
Input capacitor L=19mh	Vdc=200V	Kp=0.08 Ki=1.4	Lf=10 mH Rf=0.1Ω	Vr=300V f=50Hz	C=100μF Rp=900Ω Rs=0.001

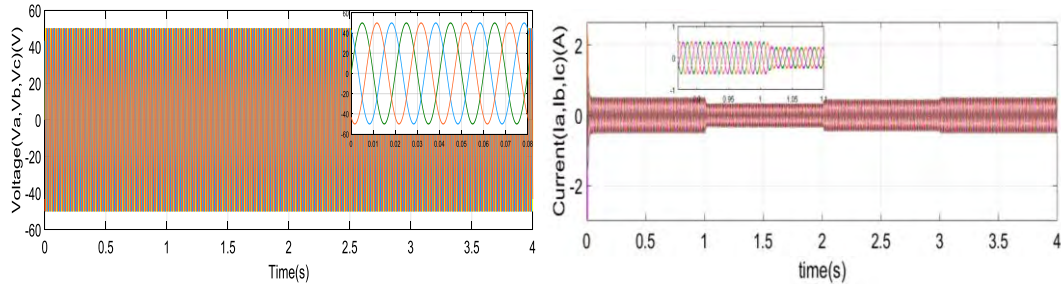


Fig 12. Network voltage and current characteristics

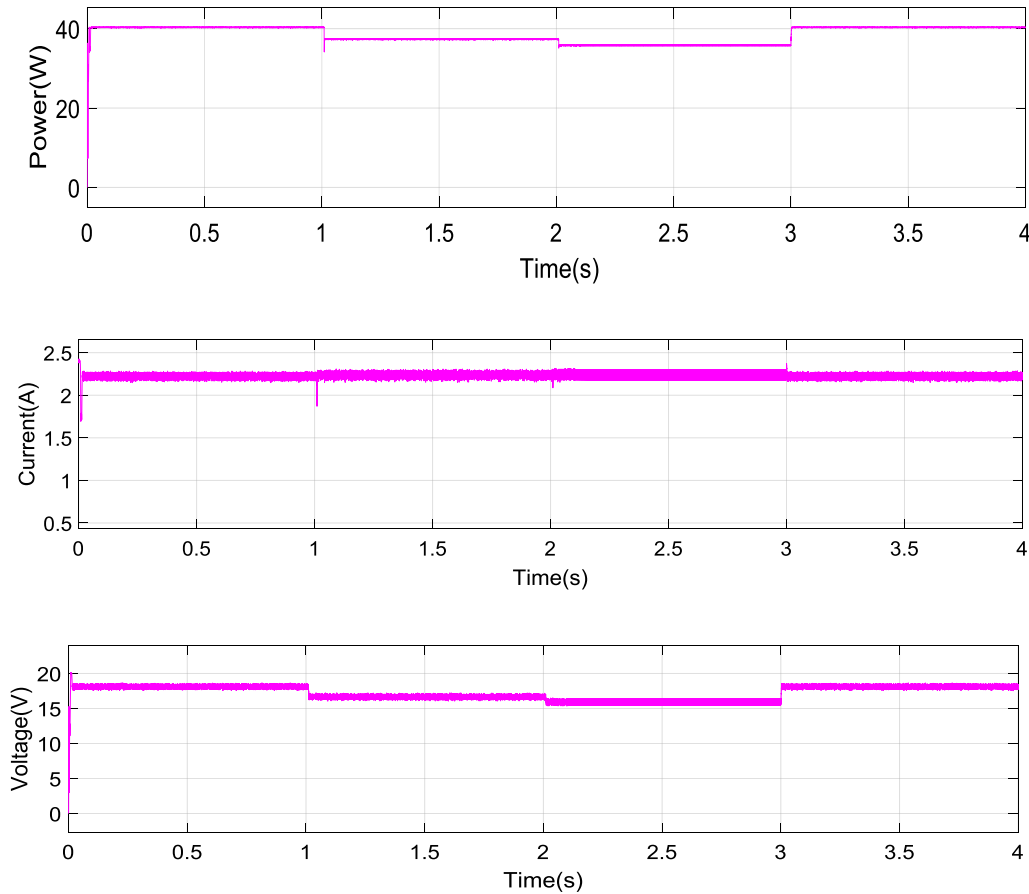


Fig 13. Temperature variations effects on the output power and voltage of photovoltaic panels

Fig. 10 shows the tracking result at a variable radiation level from 1000W/m<sup>2</sup> to 700W/M to 900W/m<sup>2</sup> and then 1000W/m<sup>2</sup>. As shown in Fig. 9, when the radiation level changes sharply within one second, the maximum power point may be promptly tracked by the MPPT controller. Furthermore, we see that all system answers include chatter. (Fig. 11) Voltage and current are delivered to the grid, and the results showed that they are affected by a change in atmospheric factors

Fig. 12 shows the temperature change. Fig. 13 exhibits how the system responds to extreme fluctuations in temperature change from (25°C, 35°C, 25 °C, 40°C). The system reaches a stable state for both

temperature levels within milliseconds. For all the above simulation results, the sliding mode control approach Simple and strong enough to withstand changing environmental conditions, fast to maintain production at an ideal level, robustness, good dynamic behavior. However, he suffers from the phenomenon of chatter, which affects the extraction of energy.

#### 4. SYNERGETIC CONTROL

The construction of a new non-linear synergetic controller is explained in this section. As a result, the design procedures for creating the synergetic controller are introduced first, followed by the fundamental ideas of this methodology. The same tests as in the preceding section are then used in a numerical simulation (Pradhan & Subudhi, 2016; Taissala et al. 2022; Chen et al. 2014; Santi et al., 2003).

Suppose a set of nonlinear differential equations of the following form describes the system to be managed.

$$\dot{x}(t) = f(x, \mu, t) \quad (15)$$

Specifies  $x$  as the state variable vector,  $\mu$  as an input controller", and  $T$  as the time vector the number of macro variables is:

$$\Psi = \Psi(x_1, x_2, \dots, x_n) \quad (16)$$

The instruction will compel the system to function at the manifold intersection (intersection for all  $\Psi = 0$ ).

The designer then chooses the macro-variable attributes (such as control output restriction, settling time, and so forth) in accordance with the control specifications. The macro-variable in the simplest instance is a straightforward combination of state variables. To define as many macro-variables as control channel numbers, the latter procedure is repeated (Sobhan, 2019; Amara et al. 2020).

The macro-variable's intended dynamic development is:

$$T_s \times \dot{\Psi} + \Psi = 0; \quad T_s > 0 \quad (17)$$

To accurately track the MPP of a DC-DC boost transformer, we must determine the instantaneous control law generated by the microcontroller MPPT, assuming that the manifold is (Bait et al. 2024):

$$\psi = \frac{\partial P_{pv}}{\partial I_{pv}} = \frac{\partial (V_{pv} I_L)}{\partial I_L} = I_{pv} \frac{\partial V_{pv}}{\partial I_{pv}} + V_{pv} = 0 \quad (18)$$

$$\frac{d\psi}{dt} = \left( \frac{\psi}{dI_L} \right) \left( \frac{dI_L}{dt} \right) \quad (19)$$

Replacing Eq. (18) in Eq. (16) gives

$$T_s \left( \frac{d\psi}{dI_L} \right) \left( \frac{dI_L}{dt} \right) + \psi = 0 \quad (20)$$

Since

$$\frac{d\psi}{dI_L} = 2 \frac{\partial V_{pv}}{\partial I_L} + I_L \frac{\partial^2 V_{pv}}{\partial^2 I_L} \quad (21)$$

When the boost converter state space equations are combined (Eqs. (8) and (20) in Eq. (19), the result is:

$$\left[ 2 \frac{\partial V_{pv}}{\partial I_L} + I_L \frac{\partial^2 V_{pv}}{\partial^2 I_L} \right] \left[ \frac{1}{L} V_{pv} - \frac{1}{L} (1-u_{pv}) V_{dc} \right] = -\frac{1}{T_s} \left[ V_{pv} + I_L \frac{\partial V_{pv}}{\partial I_L} \right] \quad (22)$$

Therefore:

$$U_{pv} = 1 - \frac{V_{pv}}{V_{dc}} - \frac{V_{pv} + I_L \frac{\partial V_{pv}}{\partial I_L}}{T_s \frac{V_{dc}}{L} \left[ 2 \frac{\partial V_{pv}}{\partial I_L} + I_L \frac{\partial^2 V_{pv}}{\partial^2 I_L} \right]} \quad (23)$$

### 4.1 Digital simulation

Simulation results obtained by the developed console They are compared with those obtained by the sliding mode controller in variable climatic conditions In order to assess the durability for the proposed control tool in MPPT under changing weather conditions, a solar insolation of 1000 W/m<sup>2</sup> is applied to the photovoltaic system. Then it is reduced to 700 W/m<sup>2</sup>, then it goes up to 900 and finally it is lift it to 1000 W/m<sup>2</sup> as shown in Fig. (9). The tracking result of this step change in both techniques is shown in Fig. 9. And the photoelectric voltage (V<sub>pv</sub>) and photoelectric current (I<sub>pv</sub>) of the synergistic controller proposed in the same step for the slider mode controller.

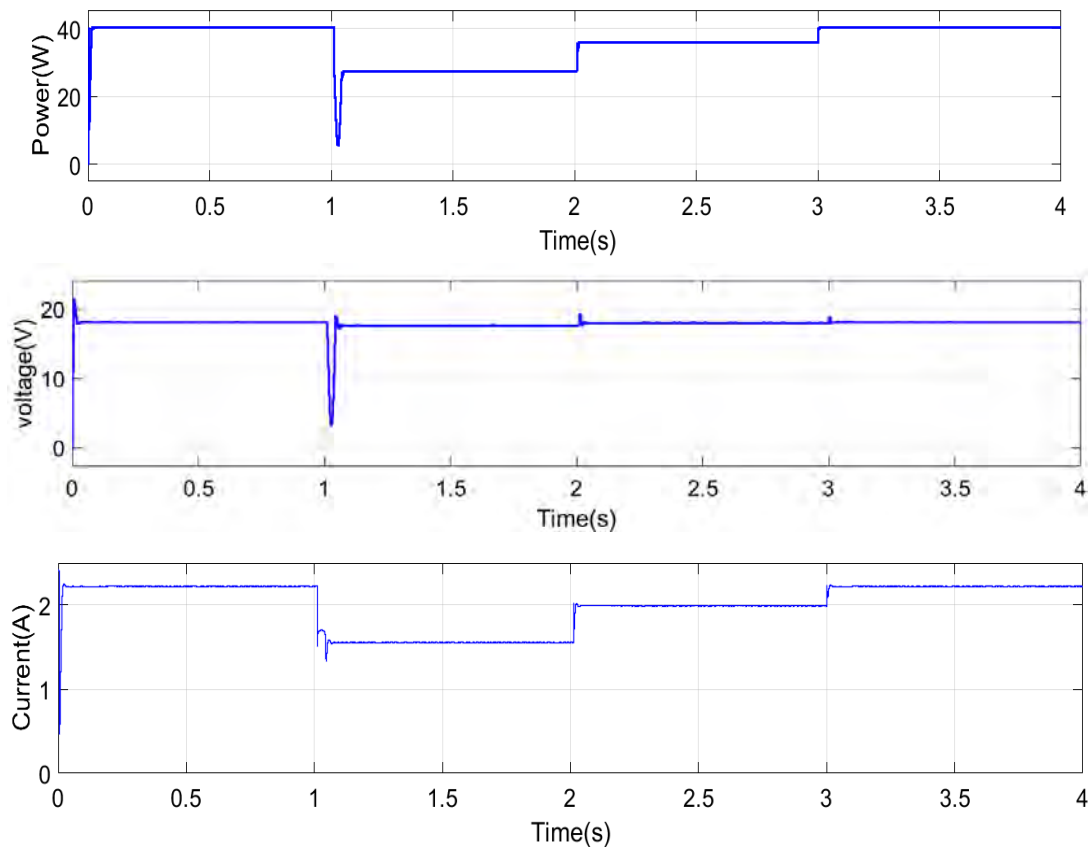


Fig 14. Simulation with step irradiance change (T=25°C)

In Fig. 14, the stability of the proposed technology, which achieved a response time of 0.002s, while the control of the sliding mode control takes a time of 0.0054 seconds, in addition, The phenomenon of chattering in the console during the control of the sliding mode can be eliminated by the proposed

technique. In the case of a constant change in atmospheric conditions, these results proved the excellent performance of the proposed control unit and high efficiency. And we can clearly note, that the synergistic approach ensures faster MPP convergence of the controller in the sliding mode and in the right direction and completely eliminates the phenomenon of chatter

To confirm that the proposed method is reliable, Figs. 15 and 16 depict the power and voltage responses of the PV system during sudden temperature changes. The data obtained demonstrate the strong flexibility of SC technology. It keeps the output power constant at MPP and tracks more accurately in less time. It is clear from the above results that the SC method clearly excels.

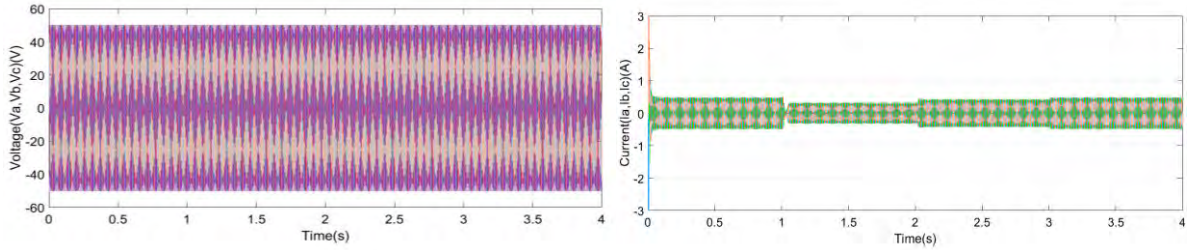


Fig. 15 Network voltage and current characteristics

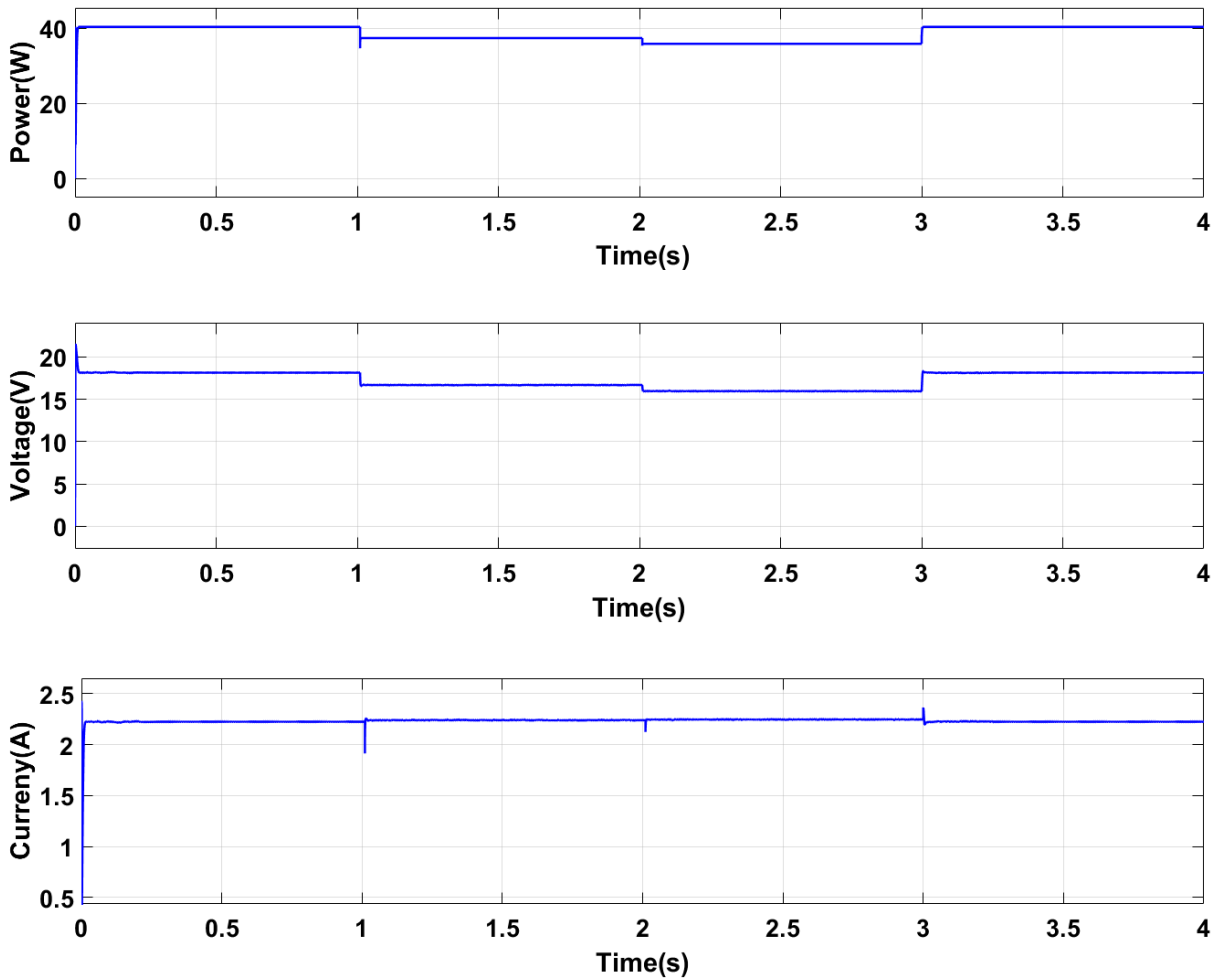


Fig. 16. Simulation with step temperature change (1000W/m2)

Fig. 17: Total energy flow, current and voltage of the extracted photovoltaic to the grid.

Fig. 18: Phase voltage, measurement and current curves Our controller tracks the MPP quickly and provides high robustness to parameter uncertainty. Furthermore, synergetic controller SC reduces oscillation around the MPP.

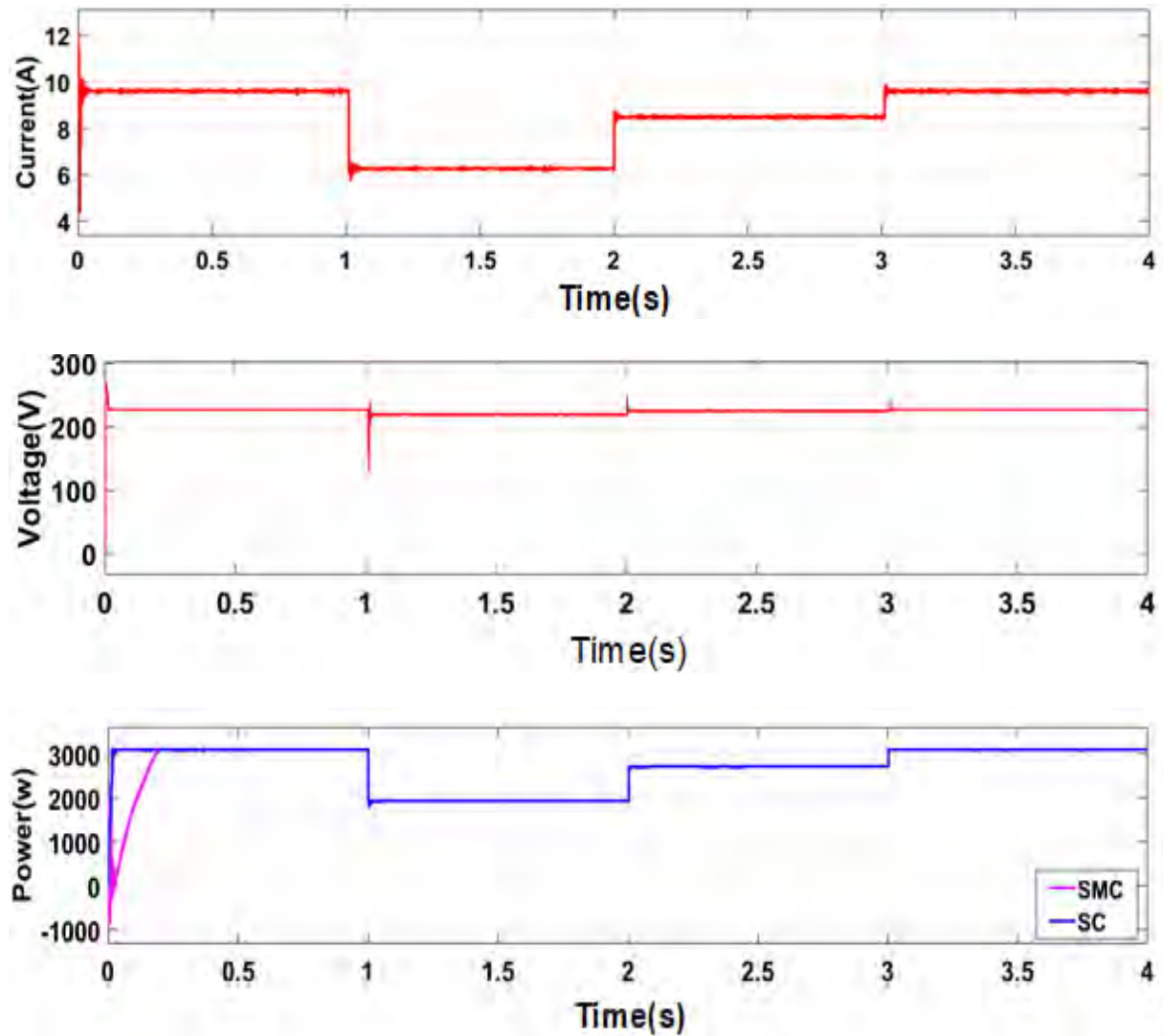


Fig 17. Voltage, current and power of the network

## 5. CONCLUSION

In order to reduce the error between the operating Capacity and maximum capacity", MPPT controllers are frequently used in solar systems to optimize the operating system performance to the maximum

In light of this research, we have presented the idea of synergetic control and put forth a novel control strategy to get rid of chattering and guarantee resilience to outside disruptions.

When the illumination changes, the SMC controller performs well and displays very strong dynamics compared to her methods, which enables it to monitor the maximum power point. But she suffers from a chattering problem that leads to loss of energy to achieve better results and eliminate the problem of chatter shown by the SMC controller. We introduced a new SC technology, where the results obtained showed its superiority over SMC in terms of stability and durability and its elimination of the problem of chatter and stability against changes in external conditions (temperature and sunlight).

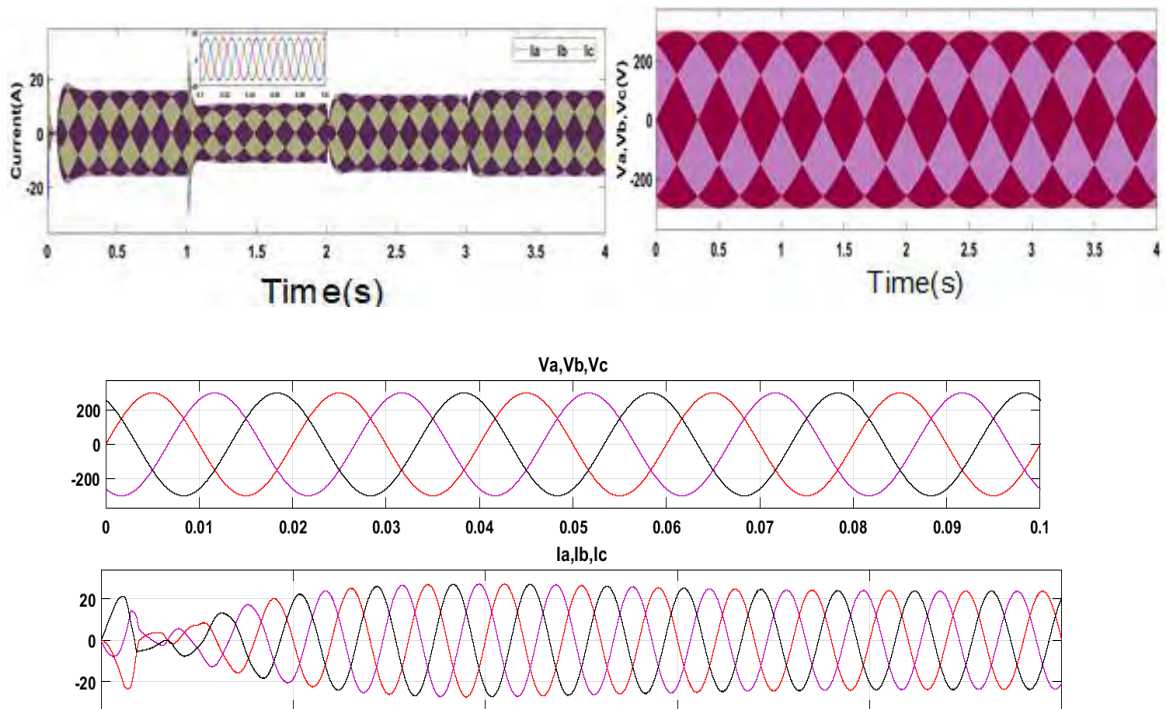


Fig 18. Phase voltage, measurement and current curves

## REFERENCES

- Ahmad FF, Ghenai C, Hamid AK, Bettayeb M. (2020). Application of sliding mode control for maximum power point tracking of solar photovoltaic systems: A comprehensive review. *Annu Rev Control*, 49:173–96. <https://doi.org/10.1016/j.arcontrol.2020.04.011>. ISSN 1367-5788
- Amara, H.E., Latreche, S., Sid, M.A. and Khemliche, M. (2020). Sliding mode observer and event triggering mechanism co-design. *Engineering, Technology and Applied Science Research*, 10(2), 5487–5491. doi: 10.48084/etasr.3285.
- Bait, F., Latreche, S. and Khemliche, M. (2022). Simulation of different faults in photovoltaic installation. 19th IEEE International Multi-Conference on Systems, Signals and Devices, SSD 2022, 1130–1138, doi: 10.1109/SSD54932.2022.9955851
- Bait, F., Latreche, S., Khemliche, M., Boulemzaoud, L. (2024). Diagnosis of a stand-alone photovoltaic installation by the Analytical Redundancy Relationship method (ARR), no. 4, 78-82. doi:<https://doi.org/10.15199/48.2024.04>
- Bouguerra, Z. & Benfdila, A. (2020). Comparative study between single and individuals mppt controller using fuzzy logic control for hybrid system (photovoltaic/wind energy conversion)” © 2021 *Advances In Electrical And Electronic Engineering*. DOI: 10.15598/aeee.v19ix.xxxx
- Bouguerra, Z. & Benfdila, A. (2023). Modelling and Simulation of PV/WECs Hybrid System Controlled by Fuzzy Logic Control. 1st International Conference on Renewable Solutions for Ecosystems: Towards a Sustainable Energy Transition (ICRSEtoSET), 979-8-3503-4633-6/23/\$31.00 ©2023 IEEE.
- Chen, J.H., Yau, H.T. and Hung, W. (2014). Design and Study on Sliding Mode Extremum Seeking Control of the Chaos Embedded Particle Swarm Optimization for Maximum Power Point Tracking in Wind Power Systems, *Energies*, 7(3), 1706-1720.

D'Souza, N.S., Lopes, L.A.C. & Liu, X. (2010). Comparative study of variable size perturbation and observation maximum power point trackers for PV systems". *Electric Power Systems Research*, 80(3), 296-305. <https://doi.org/10.1016/j.epsr.2009.09.012>

Haji D, & Gene N. (2018). Fuzzy and P&O based MPPT controllers under different conditions. In: 2018 7th International Conference on Renewable Energy Research and Applications (ICRERA). 649-655. IEEE.

Jain K, Gupta M, & Bohre A.K. (2018). Implementation and comparative analysis of P&O and INC MPPT method for PV system. In: 2018 8th IEEE India International Conference on Power Electronics (IICPE) (pp. 1-6). IEEE.

Kazmierkowski, M.P. and Sobczuk, D.L. (1996). Sliding Mode Feedback Linearized Control of PWM Inverter Fed Induction Motor', IEEE IECON, 22nd International Conference on Industrial Electronics, Control and Instrumentation, Vol. 1, 244 – 249.

Pradhan R, Subudhi B. (2016). Double integral sliding mode MPPT control of a photovoltaic system. *IEEE Trans Control Syst Technol*. 24:285–92. <http://dx.doi.org/10.1109/TCST.2015.2420674>.

Santi E, Monti A, Li D, Proddatur K, Dougal RA. (2003). Synergetic control for DC-DC boost converter: Implementation options. *IEEE Trans Ind Appl*; 39:1803–13. doi:10.1109/TIA.2003.818967.

Sobhan PV. (2019). Fast-converging MPPT technique for photovoltaic system using synergetic controller. *J Mech Contin Math Sci*. 14. <http://dx.doi.org/10.26782/jmcms.2019.12.00041>

Taissala A, Mbakop FK, Djongyang N. (2022). An optimized synergetic nonlinear controller (OSNC) based maximum power point tracking for a standalone photovoltaic system using boost converter. *SSRN Electron J*. <http://dx.doi.org/10.2139/ssrn.4012727>.